Chapter 8

The 3-D distortion effect in the Precordillera

In the previous Chapter 7, the distortion analysis of the current channeling analysis (Chapter 6) was applied to MT data of the Coastal Cordillera. It allowed the determination of a 3-D model representing the anomalous conductivity structure in the near coast region which could explain the distortion effect observed in this data. In this Chapter, the same process of distortion analysis to determine a 3-D model of anomalous conductivity will be consider for the MT data of the regions east of the Coastal Cordillera, comprising of the Longitudinal Valley (LV), the Precordillera (PC) and the Western Cordillera (WC).
The main feature to be analysed is the PC fault system, where the West Fissure is located

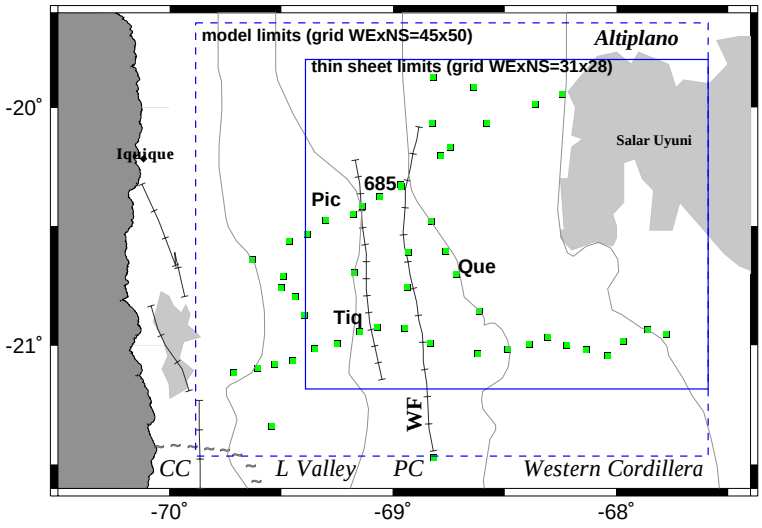

Figure 8.1: Geographical map showing the regions considered in the distortion analysis and 3-D modeling: Longitudinal Valley (*L Valley*), Precordillera (*PC*) and *Western Cordillera*. The West Fissure (*WF*) belongs to the PC fault system. Sites labeled (Tiq, Pic, 685 and Que) correspond to the data used in the study. *Blue dashed line* indicates the limits treated for the 3-D thin sheet modeling, whereas the *thick blue line* marks the area of the thin sheet.

(fig.8.1; WF). The surface contour plots of the 3-D induction strength and magnetic distortion parameters indicate the presence of an anomalous 3-D conductivity structure in the Precordillera (section 6.3.2).

The first part of this chapter (section 8.1) is an analysis of the strong distortion effect observed at some sites near the PC fault system (fig.8.1), which show anomalous phases (>90°). Using the results of the distortion analysis obtained in section 8.1, a model study is realized with a 3-D thin sheet algorithm (Weidelt [1975]). The model includes a shallow 3-D conductivity structure in the PC that explains the real induction arrows at short periods. This shallow conductor coupled with a deep conductive layer can qualitatively explain the strong magnetic distortion observed in the MT data (8.2) and the impedance phases exceeding 90°. This conductivity structure can be considered as preliminary input for a full 3-D forward modeling of the study area.

8.1 The magnetic distortion in the MT data

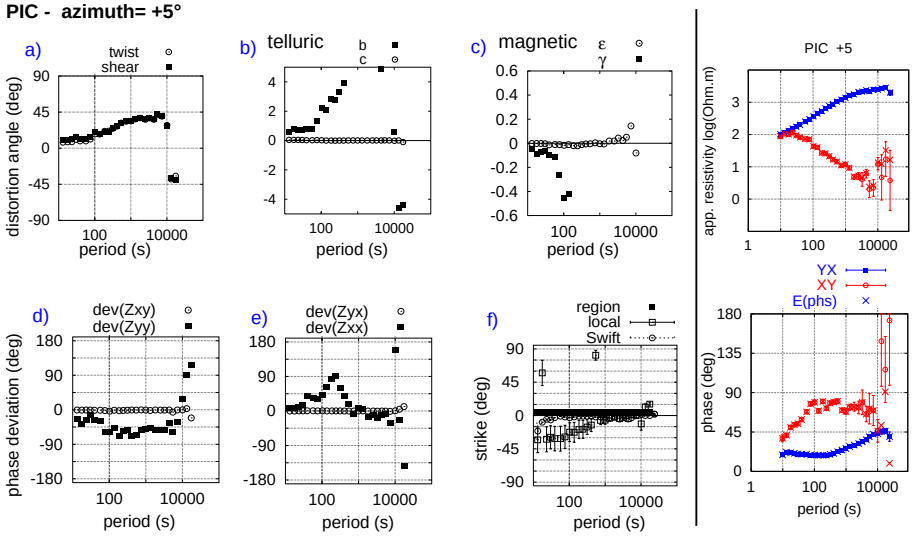

Figure 8.2: Left: Distortion parameters of the channeling analysis for site PIC, located in the Longitudinal Valley (fig.8.1). Tensor rotated by 5°N; the current channeling local azimuth at long periods. *a)* Twist and shear telluric angles, *b)−c):* Telluric (b, c) and magnetic (γ, ε) distortion parameters. *d)−e)* Phase deviations of the pairs of tensor elements. *f)* Rotation angle (5°N; *region*), current channeling *local* azimuth and the conventional *Swift* angle. In those plots where the distortion parameters b and γ surpass the usual values, they are not shown. The distortion characteristics of the *model of sub-parallel conductivity structures* are partly observed at long periods (>1000 s). *Right:* ρ_a and phase data.

The distortion parameters for the tensor rotated to the local azimuth of the current channeling (section 6.1.9), i.e., the azimuth of horizontally elongated conductor(s), are shown for four representative sites located close to the PC fault system (fig.8.1; Tiq, Pic, 685, Que). These sites are affected by strong current channeling at long periods (section 6.3.3). Site PIC from the Pica profile (20.5°S) is located west of the PC faults in the Longitudinal Valley, while site 685 is situated on the fault system. Another site (QUE) is located to the east of the faults in between the Pica and Ancorp profile (21°S). Site TIQ of the Ancorp profile is located to the west of the faults. By rotating the tensor to the local azimuth coordinate system, the TE-mode tensor elements decrease in magnitude, which in terms of the current channeling analysis correspond to the electric field components tangential to the elongated

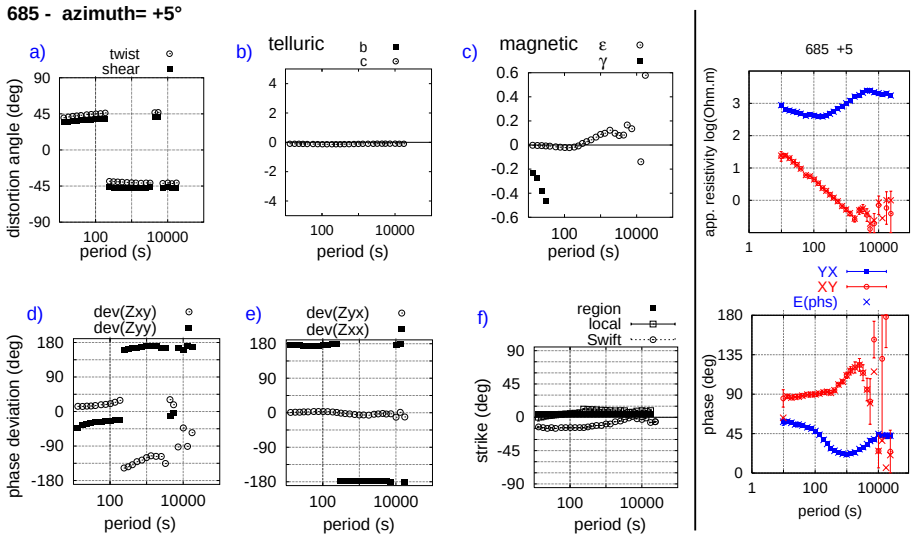

Figure 8.3: Site 685 located in the West Fissure (fig.8.1). Tensor rotated by 5°N; the current channeling local azimuth. The characteristics of the *model of sub-parallel conductivity structures* are partly observed at shorter periods. *Left:* Distortion parameters of the channeling analysis. Explanation of the plots as in fig.8.2. *Right:* ρ_a and phase data. TE-mode (XY) phases exceeding 90° at mid-long periods reflect a severe change in the current flow direction (change of sign of *twist* and *shear* deformation angles).

conductor(s).

Almost all sites affected with current channeling have local azimuths between -10 and 10°N, which is close to the direction of the faults. The exception are two sites (TIQ shown here) in Ancorp (21°S) located at the western fault system with azimuths of -50 and -40°N.

In site PIC at long periods, the tensor in the local azimuth coordinate system (5°N) shows the distortion characteristics expected for the model of sub-parallel conductivity structures (>1000 s; fig.8.2): large telluric and magnetic distortion parameters in the TE-mode (b, $\gamma >> 0$), and maximal twist and shear telluric deformation angles ($\pm 45°$). However, the phase deviations of the impedance tensor column (Z_{xy}, Z_{yy}) do not match. This means that a non neglibible induction effect exists, contradicting the assumption of DC-current on which the current channeling analysis is based.

The site on the fault system (685 in fig.8.1) rotated by 5°N (the local azimuth) is affected by strong current channeling at all periods. The distortion characteristics of the model of sub-parallel conductors partly match with the data. The change of sign of the twist and shear telluric angles at period 100 s reflects a severe change of the current flow direction, where the TE-mode phases run over 90° (fig.8.3). The equal phase deviations between the column elements (dev(Z_{xy}, Z_{yy})) are not achieved, which means that induction effects are not negligible. The magnetic parameter (ε=e) of the TM-mode does not vanish at long periods, indicating a departure from the hypothesis of sub-parallel conductivity structures at the corresponding penetration depth.

For sites TIQ and QUE further south (fig.8.1), the distortion characteristics of the model of sub-parallel conductors fit poorly with the data. The current channeling, however, is strong (maximum shear), and an inductive effect is observed especially at longer periods, where the magnetic distortion increases with period (frequency dependent magnetic parameters (ε, γ).

Thus neither a -10°N local azimuth to the southeast (QUE; fig.8.4) nor a -40°N to the southwest (TIQ; fig.8.5) of the fault system support a model of sub-parallel conductivity structures at these locations. On the other hand, if the regional strike were N-S, then site TIQ, with a -40°N local azimuth, will never fit with the model of sub-parallel structures. A strong change in the current flow direction is also observed at these sites at mid-periods, expressed in a change of sign of the twist and shear angles and in the TE-mode phases >90° (figs. 8.4, 8.5; right).

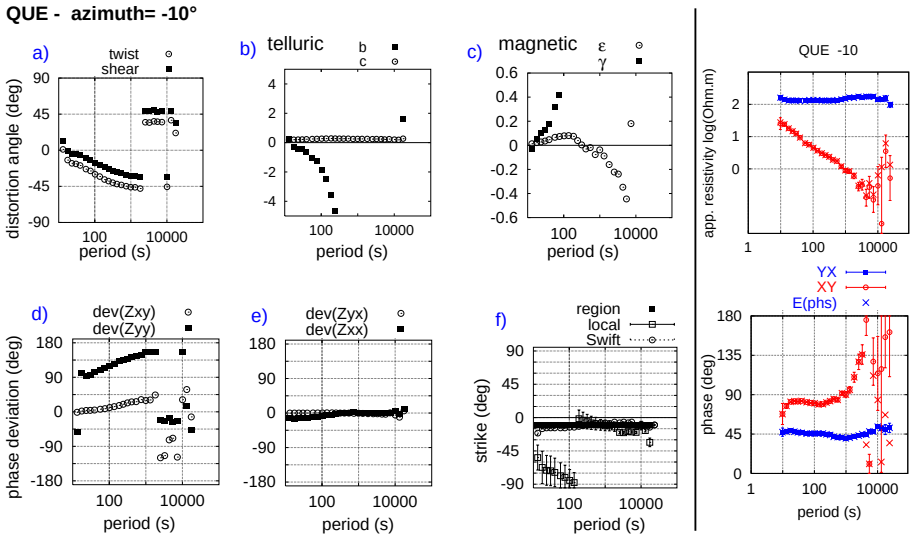

Figure 8.4: Site QUE located east of the West Fissure zone (fig.8.1). Tensor rotated by -10°N; the current channeling local azimuth at periods >100 s. *Left:* Distortion parameters of the channeling analysis. Explanation of the plots as in fig.8.2. *Right:* ρ_a and phase data. TE-mode (XY) phases exceeding 90° at long periods reflect a severe change of the current flow direction (change of sign of *twist* and *shear* deformation angles).

The most important result of the distortion analysis is that a model of sub-parallel conductivity structures can not satisfactorily explain the MT data. Instead, a 3-D structure not necessarily consisting of elongated conductors seems more suitable to explain the strong telluric and magnetic distortions observed. Because at short periods the local magnetic distortion is not negligible and the induction arrows behave in a 3-D manner, a shallow 3-D conductive structure in the PC might be present.

8.2 3-D thin sheet modeling

In this section the local conductivity structure is examined qualitatively by means of 3-D thin sheet modeling. The forward model algorithm of Weidelt [1975] is used to investigate whether an anomaly such as a simple 3-D thin sheet conductor embedded in a layered earth can reproduce such magnetic distortion and inductive effects as were observed in the field data.

The background (i.e., regional) model is restricted to a 1-D layered model, and the 3-D thin sheet conductor can be placed at any depth within a layer. The sheet has only physical

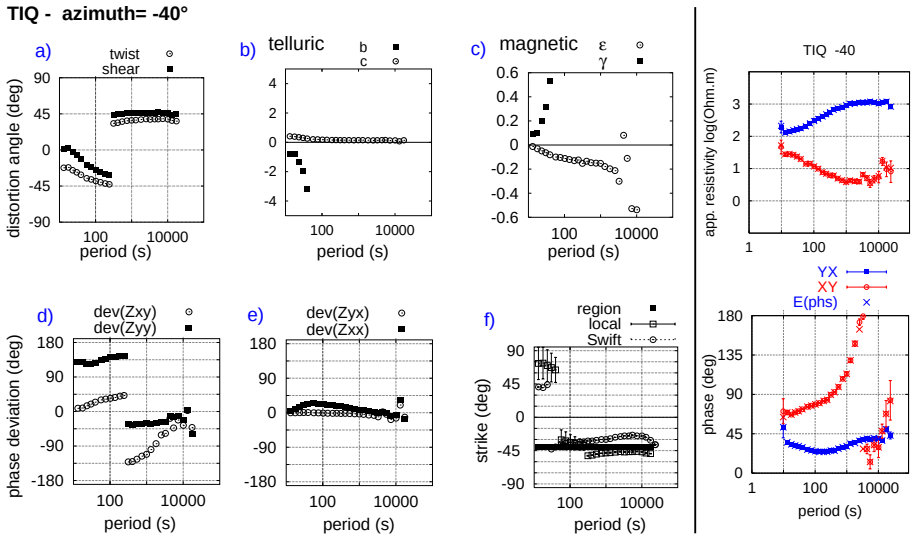

Figure 8.5: Site TIQ located west of the West Fissure zone (fig.8.1). Tensor rotated by -40°N; the current channeling local azimuth at periods >100 s. *Left:* Distortion parameters of the channeling analysis. Explanation of the plots as in fig.8.2. In those plots where the telluric (b) and magnetic (g=γ) distortion parameters are not seen is because they surpass the usual limits. *Right:* ρ_a and phase data. TE-mode (XY) phases running over 90° at long periods reflect a severe change of the current flow direction (change of sign of *twist* and *shear* deformation angles).

thickness. Mathematically, it is assumed to vanish, while its conductivity approaches an infinite value. Using this approach ensures that the regional field components at the external boundaries of the thin sheet remain unchanged, provided that certain boundary conditions are achieved. The first boundary condition is that the sheet thickness should be much less than the skin depth of the induced fields[1] (Weaver [1994]). The second condition is that the penetration depth of the fields beneath the sheet is much greater than its thickness. This means that the construction of the model is controlled by the sheet conductance ($\int \sigma \cdot dz$ $[S]$), which is the conductivity (σ $[S/m]$) integrated over a certain depth range (dz $[m]$). A sheet with a conductance of 1000 S, for example, would correspond to a layer with a conductivity of 1 S/m and a thickness of 1000 m. Subject to the sheet depth and conductances, a minimum period for the model responses and hence a minimum penetration depth should be considered to satisfy the boundary conditions.

The models presented here were constructed taking these conditions into consideration. For the conductivity and conductance values of models A and B (figs. 8.6, 8.7), it was found numerically that a valid forward solution is achieved at period >50 s.

Two different background conductivity models (i.e., 1-D layered model) are considered to analyze induction and anomalous magnetic effects in the responses of MT data. Both models include a shallow layer with a thickness of 9 km and a resistivity of 500 Ωm, simulating normal resistivity values for the upper crust. Model A includes layers with lower resistivity values in depth than model B (fig.8.6). Model A can be associated with a lithosphere of normal resistivity values, with a mantle layer of 20-50 Ωm below 300 km depth, while model (B) represents a thinner lithosphere with a more conductive mantle (10 Ωm) below 120 km

[1]The skin depth in the sheet is $\sqrt{2}\frac{1}{\sqrt{w\mu_0\sigma}}$, where μ_0 is the magnetic permeability of the vacuum, w the circular frequency and σ the conductivity of the sheet.

depth, likelier to exist in orogone zones.

The 3-D thin sheet structure, comprising the Pre- and Western Cordillera (fig.8.1), was determined by trial and error, through searching to fit the induction arrows at short periods (100 s). The induction arrows were corrected of the ocean effect[2] (Section 9.1). The best fit was found for the sheet at a depth of 2 km. The model shows higher E-W average conductances in the north of the Precordillera than in the south (fig.8.7). The sheet extends to the east with higher integrated conductivities in the western limits of the Altiplano (fig.8.7) in order to simulate a highly conductive sedimentary layer, as was derived by the 2-D inversion modeling of Ancorp data (Schwalenberg, 2000).

Comparison of the real parts of the induction arrows for the period 100 s of the data and responses of the thin sheet model can be seen in fig.8.7. The data from the Longitudinal Valley and the Precordillera fit well with the model responses. The induction arrows of model A and B (fig.8.6) at period 100 s are equivalent because the penetration depth of the EM fields are at the levels of the thin sheet. This modeling study is not intended to find a best fit for the induction arrow data in the Western Cordillera (fig.8.7), since it is known that the conductor to the east should extend further into the hearth of the Altiplano (section 9.2). This can not be modeled properly due to limitations in the maximum grid size.

3-D images of the induction

The 3-D images of the distortion parameters of the measured MT data (Section 6.3.2) are compared with that from the model responses. The parameters are 3-D induction strength (Section 6.1.8) and magnetic distortion, calculated over the period ranges 50-1000 s and 1000-6000 s at single sites. The magnetic distortion parameters (ε, γ) are related to the deviation of the regional magnetic fields from their coordinate system due to the anomalous DC magnetic fields produced by the local 3-D structure (Smith [1997]).

The contour plots of the images at the short period band are illustrated in fig.8.8 for model

[2]The ocean effect removal was a correction valid at short periods. At longer periods the induction arrows are seen to be coupled with the ocean.

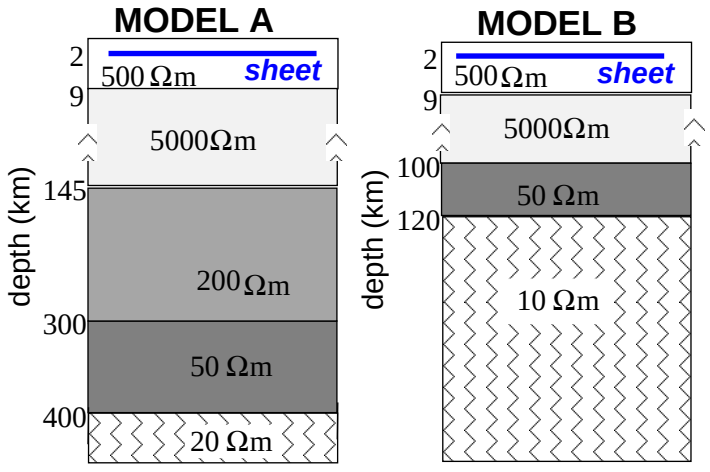

Figure 8.6: Vertical cross section of the 1-D layered (background) models considered in the 3-D thin sheet algorithm. The thin sheet (horizontal blue line) lies at 2 km depth, embedded in the first layer. Model A represents a normal lithosphere and Model B a thinner lithosphere with a low resistive layer (10 Ωm) below 120 km representing the mantle.

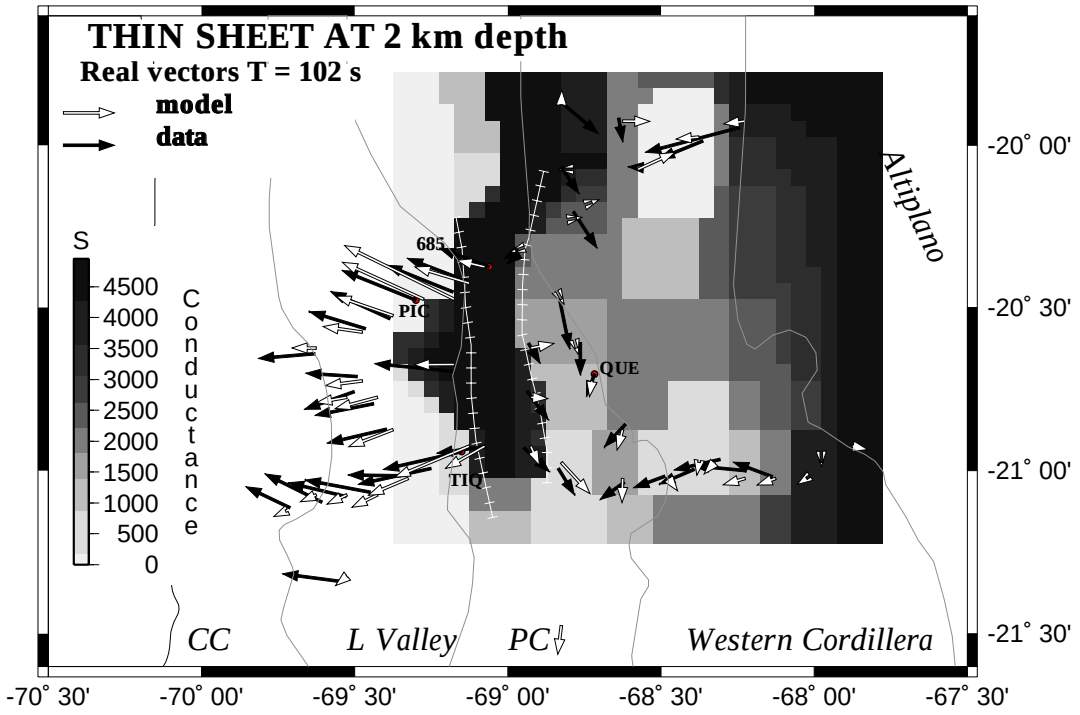

Figure 8.7: Horizontal view of the 3-D thin sheet structure in conductance values at a depth of 2 km. The 1-D background resistivity models are shown in fig.8.6. Modeled real induction arrows (white) are compared with the data (black) which have been corrected of the ocean effect (period 100 s). The sites labeled are used in the current channeling analysis (figs.8.2 to 8.5).

A and the observations. The images of model A and B (fig.8.6) at the short period band are equivalent, reflecting that the EM fields are not affected by the deeper layers. Thus, the greater 3-D induction strengths and the magnetic distortions seen in the contour plots of the models (fig.8.8; bottom) is due solely to the effect of the thin sheet anomaly. However, the 3-D induction strength of the models responses in the Precordillera is much smaller than that of the field data (fig.8.8a), while the magnetic distortion of the latter is comparable to that of the models (fig.8.8b). The measured data are affected by a greater inductive 3-D anomaly. This suggests that a more complicated structure exists in depth as is indicated by the background models (fig.8.6).

The distortion images of the model responses at the long period band (1000-6000 s) show greater differences between model A and B. While the induction effect produced by the thin sheet has almost vanished for model A (3-D induction strengths vanish), it is still significant for model B (fig.8.9a). If the low resistivity (10-20 Ωm) bottom layer is moved to a shallower depth (from 400 to 120 km depth; models A, B in fig.8.6) a coupling effect between the bottom layer and the 3-D thin sheet becomes evident[3].

The magnetic distortion effect increases in both models with period, similarly to the measured data (fig.8.9b). The increment is larger in model B (bottom layer at 120 km) than in A (bottom layer at 400 km), reflecting again the greater coupling effect with the bottom layer set at shallower depth (B).

[3]The skin depth for the period 5000 s in model A is 192 km and model B, 148 km, considering a sheet with a resistivity of 0.5 Ωm and a thickness of 2 km (=4000 S).

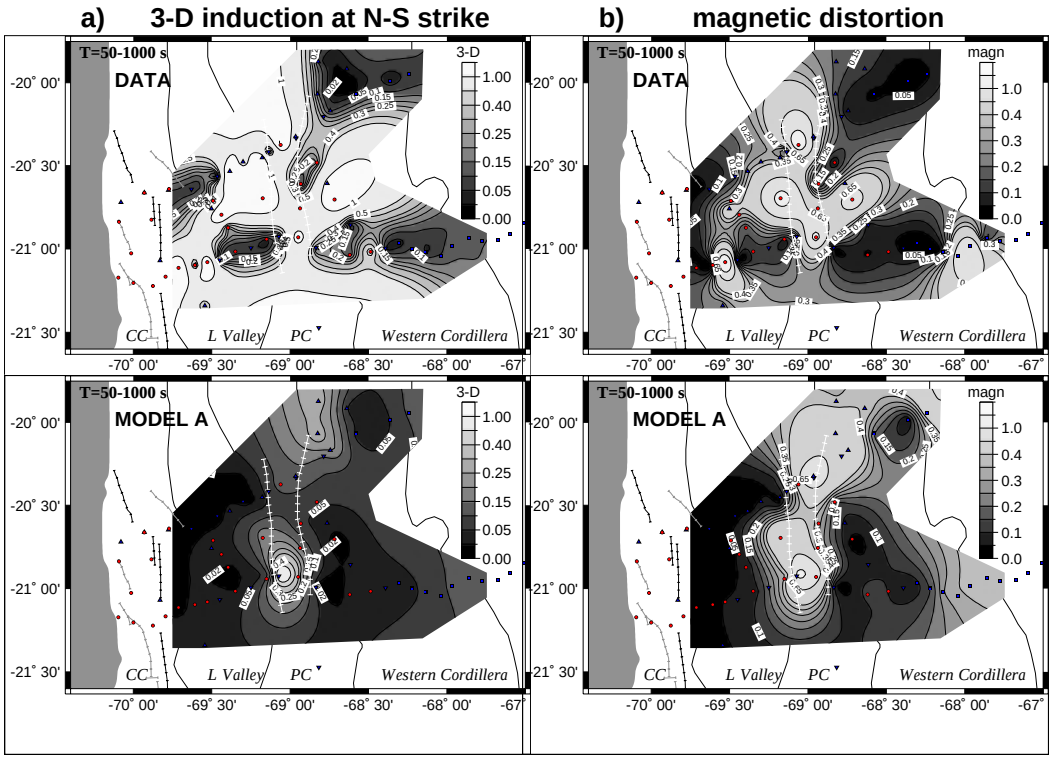

Figure 8.8: Interpolated site average parameters of the distortion analysis for the data (*above*) and the model response (*below*) treated in the N-S coordinate system at the period band 50-1000 s. The 3-D thin sheet is the anomaly for the model source of the distortion. *a)* 3-D induction strength; light grays-white are indicative of non negligible induction effects. *b)* Magnetic distortion, related to the deviation of the regional magnetic fields from the N-S coordinate system due to the anomaly.

If the low resistivity bottom layers are completely removed from the models, then the magnetic distortion (as a measure of the regional magnetic field deviations due to the anomaly) should decay with the period, as predicted by the galvanic distortion hypothesis.
The responses of Model B are closer to the 3-D induction effect observed in the Precordillera, suggesting that a conductive layer exists in depth.

8.3 Model interpretation

The images of the distortion parameters have shown that a local anomaly like that of the 3-D thin sheet model is the cause of the local magnetic distortion observed in the Precordillera. However, the 3-D thin sheet model alone does not attain the magnitude of the observed 3-D induction strength at long periods in the Precordillera.
Model B (fig.8.6) is closer to the observations, suggesting that *a high conductivity zone further in depth must exist to explain the greater 3-D induction strengths and magnetic distortion observed at longer periods.*

In the following we will concentrate on the model responses of one particular site which show strong distortion affected with current channeling at long periods, similar to the observations.

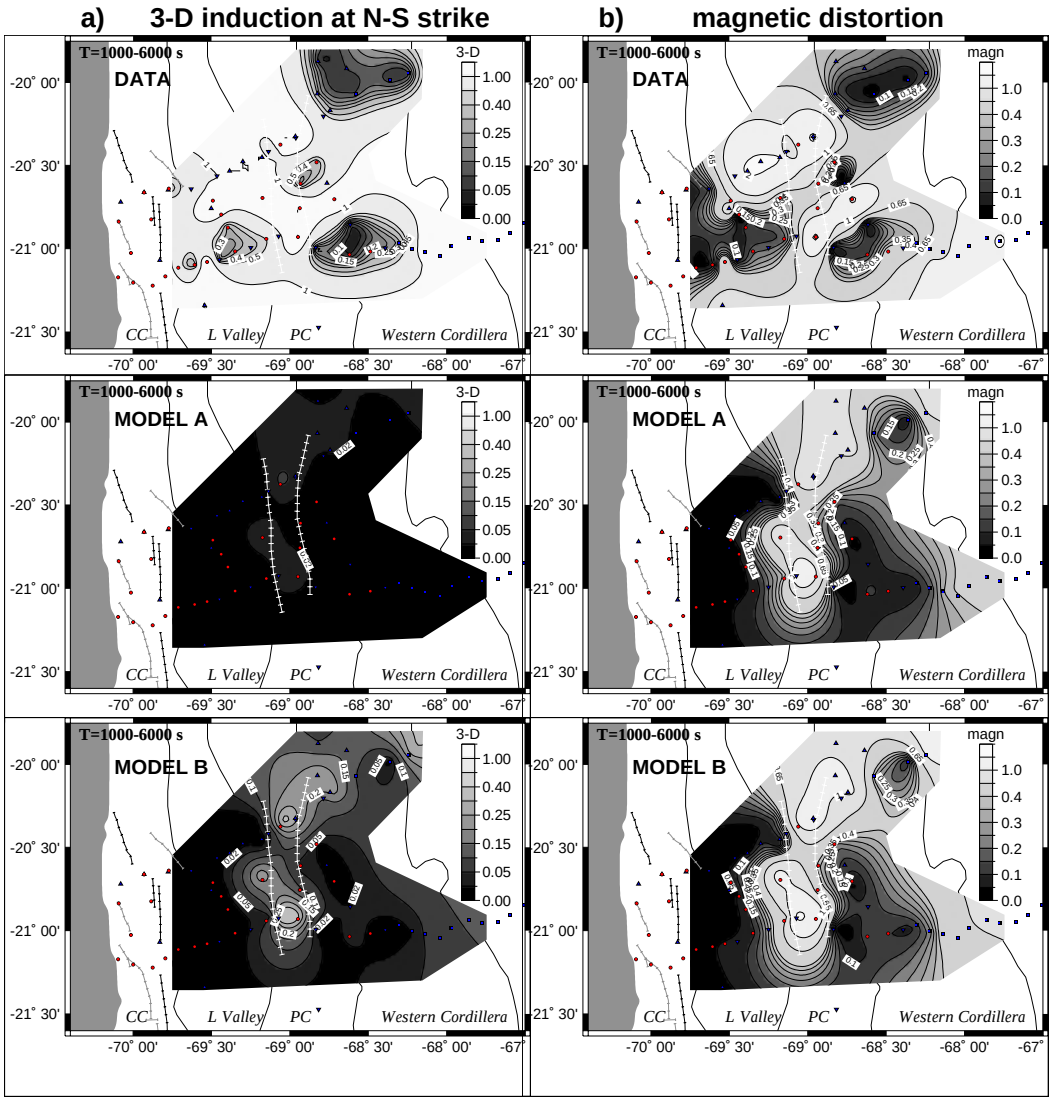

Figure 8.9: Interpolated site average parameters of the distortion analysis for the data (*above*) and the model responses (A; *center*, B; *below*) treated in the N-S coordinate system at the period band 1000-6000 s. For the models, the location of the 3-D thin sheet (the anomaly) is shown in fig.8.7 . *a)* 3-D induction strength; light grays-white are indicative of non negligible induction effects. *b)* Magnetic distortion, related to the deviation of the regional magnetic fields from the N-S coordinate system due to the anomaly.

The site is located above the northwest boundary of the thin sheet model (fig.8.7; PIC). The distortion analysis was applied at this site to the MT data of both model responses, for the tensor rotated by 20°N, 90° from the current channeling local azimuth (-70°N). The telluric deformation angles (twist and shear) are almost equal between both models (figs. 8.10, 8.11), while the magnetic parameter of the TE-polarisation (g=γ) is greater at long periods for model B (with the shallower bottom layer; fig.8.11), as has been already observed in the 3-D images of the long period band (fig.8.9).

At the period band 100-1000 s the strongest inductive effect is observed, seen in the frequency dependence of the distortion parameters (figs. 8.11, 8.10). For model B, the anomalous TE-mode phases >90° has occurred at this period range (fig.8.10), whereas for model A (the deeper bottom layer; fig.8.11), the TE-mode phases are near but not exceeding 90°. Also, ρ_a

is fairly smaller for model B, reflecting a smaller electric field amplitude for the component parallel to the local azimuth.

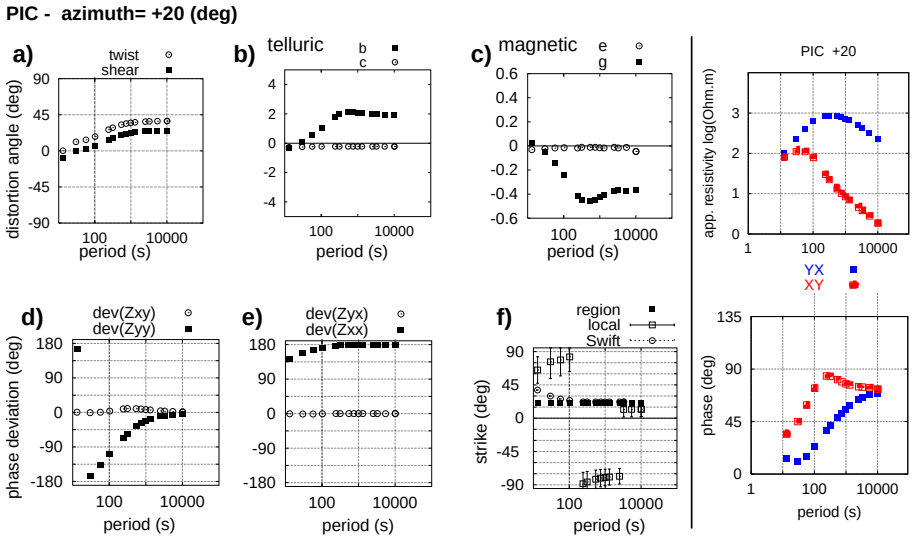

Figure 8.10: Site PIC located in the Longitudinal Valley (LV; fig.8.7) with the response of model A (fig.8.6). Tensor rotated by 20°N; the current channeling local azimuth with 90° added. *Left:* Distortion parameters of the channeling analysis. Explanation of the plots as in fig.8.2. *Right:* ρ_a and phase data.

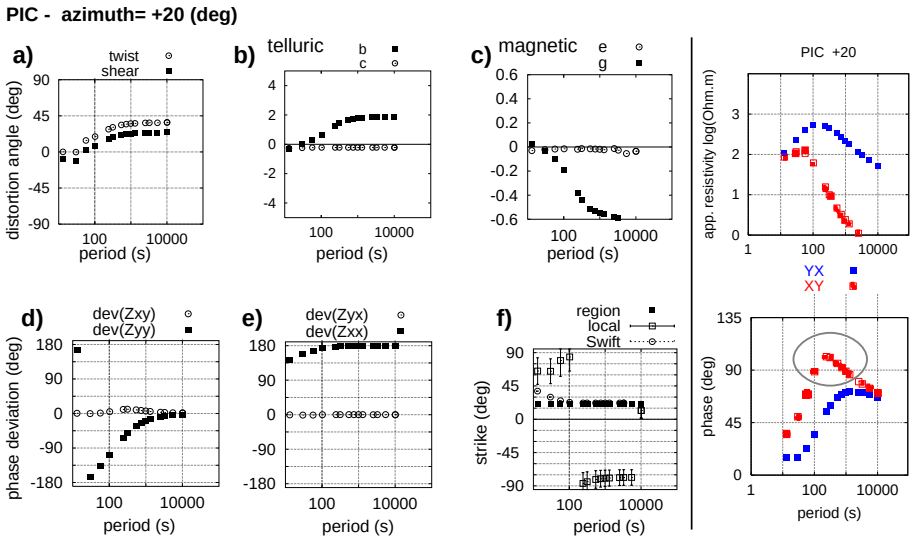

Figure 8.11: Site PIC located in the Longitudinal Valley (LV; fig.8.7) with the response of the model B (fig.8.6). Tensor rotated by 20°N; the current channeling local azimuth with 90° added. *Left:* Distortion parameters of the channeling analysis. Explanation of the plots as in fig.8.2. *Right:* ρ_a and phase data. TE-mode (XY) phases running over 90° at mid periods (100-1000 s) reflect a severe change in the current flow direction.

In chapter 7, for the 3-D model with an elongated conductor striking differently from a 2-D block simulating the ocean, phases >90° occur coinciding with a change of sign of the telluric deformation angles (twist and shear), reflecting a significant change of the current flow direction. A similar situation is observed at site PIC of model B (fig.8.11). At period 100 s there is a change in sign of the twist and shear angles, and the TE-mode phases

increase beyond 90°. The TE-mode phases exceeding 90° at periods 100-1000 s in model B suggest that the coupling effect between the shallow 3-D thin sheet anomaly and the deeper conductive layer causes a severe change in the current flow direction at the corresponding penetration depths[4].
While the TE-mode phases >90° of model B in the period band 100-1000 s reflect a coupling effect, at longer periods these correspond to the response of the 1-D background model (PIC; fig.8.11). In contrast, the observed TE-mode phases always increase with period, surpassing 90° at periods >500 s (figs. 8.3, 8.4, 8.5), whereas the TM-mode phases of the model decrease with period. This clearly indicates that a deep 2-D (or 3-D) structure exists in the Precordillera.

8.4 Summary of the 3-D distortion effect

An interpretation of the distortion analysis applied to both the model responses and the field data of the Precordillera are summarized below:
1) The 3-D anomaly must start at shallow depths (∼2 km) in order to explain the behaviour of the induction arrows at short periods as well as the strong local magnetic distortion observed in the MT data.
2) A deeper high conductivity zone is necessary to explain the 3-D induction strength and magnetic distortion effects with increasing period.
3) Anomalous phases (>90°) can occur for EM-fields observed close to a high 3-D conductivity contrast near the surface (site PIC; fig.8.7), at the penetration depths where a severe change in the current flow direction occurs, as a product of the coupling between a conductive deeper layer and the sharply shallower anomaly.
4) To determine whether the local anomaly and the deeper conductor are connected or how are they distributed with respect to each other requires a full 3-D model study.

[4]The skin depths of model B at periods 100 and 1000 s are 6 km and 43 km, respectively, while the real part of the EM-wave propagation response (C) is 2.7 and 9 km, respectively.